^{15}N spin-relaxation studies of N_2 in buffer gases. Cross sections for molecular reorientation and rotational energy transfer

Cynthia J. Jameson
Department of Chemistry, University of Illinois at Chicago, Chicago, Illinois 60680

A. Keith Jameson
Department of Chemistry, Loyola University, Chicago, Illinois 60626

Nancy C. Smith
Department of Chemistry, University of Illinois at Chicago, Chicago, Illinois 60680

(Received 19 December 1986; accepted 5 March 1987)

Nuclear spin-lattice relaxation times (T_1) have been measured as a function of temperature for ^{15}N in N_2 gas and in CH_4, O_2, CO, Ar, HCl, CF_4, Kr, and Xe. The relaxation is dominated by the spin-rotation mechanism so that empirical values of the cross sections for rotational angular momentum transfer (σ_J) are obtained as a function of temperature. The values of $\sigma_J/\text{Å}^2$ at 300 K are 13.6 ± 0.4 (N_2–CH_4), 14.9 ± 0.4 (N_2–N_2), 14.7 ± 0.6 (N_2–O_2), 15.0 ± 0.9 (N_2–CO), 15.9 ± 0.8 (N_2–Ar), 22.7 ± 0.6 (N_2–HCl), 30 ± 1 (N_2–CF_4), 18.1 ± 0.5 (N_2–Kr), and 19.8 ± 0.5 (N_2–Xe). For almost all cases, the temperature dependence of the cross section deviates from T^{-1}.

INTRODUCTION

Nuclear spin relaxation in the gas phase is due entirely to the anisotropy of the intermolecular potential. Such studies can be interpreted in terms of a single cross section for rotational angular momentum transfer which may be used for the refinement of intermolecular potentials. N_2 has been chosen for relaxation studies for several reasons. N_2 is an important component of the atmosphere. The N_2–N_2 diatomic pair is the simplest homonuclear diatomic pair excepting H_2–H_2. While a fully quantum scattering treatment is needed in treating H_2–H_2 collisions because the rotational energy levels are so widely spaced, N_2–N_2 collisions may be treated classically or semiclassically. ^{15}N in N_2 has a single relaxation mechanism (spin-rotation) in the gas phase, allowing collision cross sections of a specific type to be extracted from ^{15}N relaxation times.

A wide variety of effective cross sections are available for the N_2 molecule, and the behavior of the different cross sections with temperature or with rotational quantum number has been discussed.[1] By means of the Waldmann–Snider equation (the quantum mechanical analog of the Boltzmann equation) a unified description of various experiments has been formulated.[2] Each effect has been associated with a particular combination of effective cross sections which identify specific microscopic collisional processes giving rise to the observable. For N_2–N_2, the available data have been used together so as to yield empirical values of various effective cross sections.[1] Furthermore, there are trajectory calculations of these cross sections, using an assumed potential which has been previously optimized via a multiproperty analysis of pure N_2 in the solid state, and tested by comparison against other observables such as second virial coefficients and gas transport properties.[3]

A definitive theoretical N_2–N_2 interaction potential is not yet available, although *ab initio* calculations of both the short-range and long-range parts have been published.[4] Properties calculated with the *ab initio* potentials of Berns and van der Avoird or the electron-gas potential of van Hemert and Berns[4] differ significantly from experimental values at all temperatures for second virial coefficients, viscosity coefficients, and other observables.[5] A potential resulting from a combination of the short-range term from the *ab initio* SCF calculations, a long-range multipole expansion, and a damping term obtained by fitting to $(N_2)_2$ dimer structure, second virial coefficients, and solid properties is still deficient in predicting bulk properties.[6] The newest *ab initio* calculations yield results of lesser quality for several experimental observables. Only when two empirical scaling parameters are introduced does this potential reproduce second virial coefficients over a wide temperature range and give a closer fit to experimental data on several properties of solid nitrogen.[6]

Some recent data on pure N_2 include more accurate PVT measurements,[7] second structural virial coefficients from neutron scattering,[8] and mean square torques from second moments of Rayleigh and Raman lines.[9] Collision-induced far infrared and microwave absorption in N_2 gas yield experimental values for the electric quadrupole and octopole moments.[10]

N_2–rare gas interactions are also of interest as three-atom potentials similar to H_2–rare gas systems in complexity but providing the advantage of closely spaced rotational levels and an intermediate mass in N_2 compared to the rare gas sequence. Data on these systems include broadening of rotational Raman lines of N_2, diffusion coefficients, and the effects of a magnetic field on binary diffusion.[11]

The present work provides the first spin-relaxation studies in $^{15}N_2$ in various buffer gases and complement the ^{14}N quadrupolar relaxation studies in pure $^{14}N_2$.[12] Earlier relaxation studies in pure $^{15}N_2$ gas were linewidth measurements which give relaxation times of lower accuracy since

 0021-9606/87/126833-06$02.10

the lines are fairly narrow for $^{15}N_2$, as opposed to $^{14}N_2$.[12] We find temperature dependent cross sections for N_2 collisions with N_2, CH_4, O_2, CO, Ar, HCl, CF_4, Kr, and Xe.

EXPERIMENTAL

The gas samples were prepared as in our previous studies of the temperature and density dependence of the nuclear shielding,[13] using isotopically labeled ($>90\%$ ^{15}N) $^{15}N_2$ gas from MSD Isotopes. Buffer gases were not isotopically labeled and were used as obtained from vendors.

Measurements were made at 20.28 MHz at 4.7 T on an IBM WP-200 NMR spectrometer. The mode of operation at variable temperature has been described previously[14] using the standard inversion recovery pulse sequence $[5T_1\text{-}\pi\text{-}\tau\text{-}\pi/2]_n$.[15] Integration of Bloch's equations lead to intensities proportional to bulk magnetization along the applied magnetic field which vary with the delay time τ as follows:

$$A_\tau = A_\infty\,[1-\exp(-\tau/T_1)] + A_0\exp(-\tau/T_1). \qquad (1)$$

The above form accounts for any slight deviation from the optimum $A_0 = -A_\infty$ owing to B_1 (rf) field inhomogeneity. Typical plots of $\ln[(A_\infty - A_\tau)/(A_\infty - A_0)]$ vs τ are shown in Fig. 1. Densities used in this study (5–50 amagat) are all in the "extreme narrowing limit" (collision frequency is large compared to the Larmor frequency of the spin) where spin-lattice relaxation times are proportional to density ρ.

A characteristic $(T_1/\rho)_{N_2\text{-buffer}}$ may be extracted from T_1 of the mixture

$$T_1 = (T_1/\rho)_{N_2\text{-}N_2}\rho_{N_2} + (T_1/\rho)_{N_2\text{-buffer}}\rho_{buffer}, \qquad (2)$$

since the relaxation mechanism is purely spin rotation for ^{15}N in N_2. The form of Eq. (2) has been established by our spin-relaxation studies of ^{13}C in CO_2 with various buffer gases.[14] The experimental temperature dependence of (T_1/ρ) is adequately described by

$$(T_1/\rho) = (T_1/\rho)_{300\,K}(T/300)^{-n}. \qquad (3)$$

TABLE I. Spin-relaxation times for ^{15}N in N_2 with various buffers.[a] $(T_1/\rho) = (T_1/\rho)_{300\,K}\,(T/300)^{-n}$.

Buffer	$(T_1/\rho)_{300}$ (ms amagat^{-1})	n
CH_4	2.42 ± 0.07	1.10 ± 0.06
N_2	2.23 ± 0.06	1.20 ± 0.03
O_2	2.16 ± 0.08	1.37 ± 0.06
CO	2.3 ± 0.1	1.17 ± 0.09
Ar	2.2 ± 0.1	1.24 ± 0.04
HCl	3.22 ± 0.08	1.48 ± 0.02
CF_4	3.6 ± 0.2	1.38 ± 0.04
Kr	2.23 ± 0.07	1.24 ± 0.05
Xe	2.31 ± 0.06	1.27 ± 0.05

[a] Temperature range is 260–400 K for N_2 in CH_4, HCl, and Xe, 225–400 K for N_2 in O_2, CO, CF_4, and Kr, and 215–400 K for pure N_2 and N_2 in Ar.

RESULTS

Table I shows the temperature dependence of T_1/ρ for each N_2/buffer pair differs significantly from $T^{-3/2}$ in each case. A typical plot is shown in Fig. 2. It is specially interesting that the relaxation time of the N_2–O_2 pair is not unusually short and increases linearly with O_2 density in the 5–40 amagat regime just like the other N_2-buffer pairs. This indicates that the spin-rotation mechanism in N_2 is very efficient, and that it is not possible to separate out any intermolecular dipole–dipole interaction between the ^{15}N nucleus and the unpaired electron spins in O_2. Even in this paramagnetic gas the $^{15}N_2$ relaxation is dominated by the spin-rotation mechanism.

Cross sections for angular momentum transfer at 300 K in Table II were calculated from the measured (T_1/ρ) using

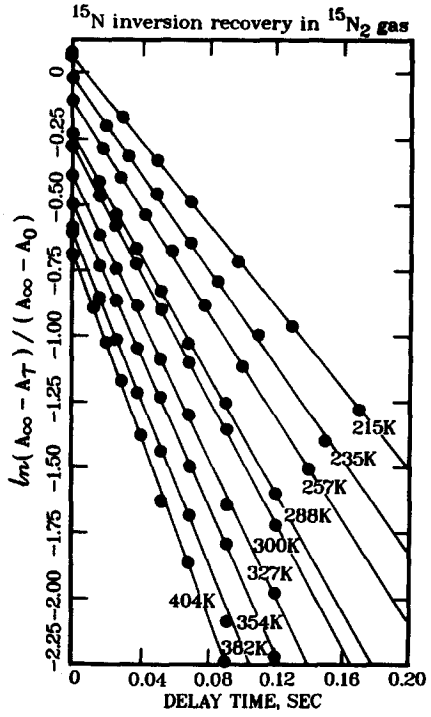

FIG. 1. Typical inversion recovery data for ^{15}N in pure N_2 gas (38 amagat). (The ordinate of each line has been displaced so that all curves may be displayed in the same plot.) The slope of each line is $-1/T_1$.

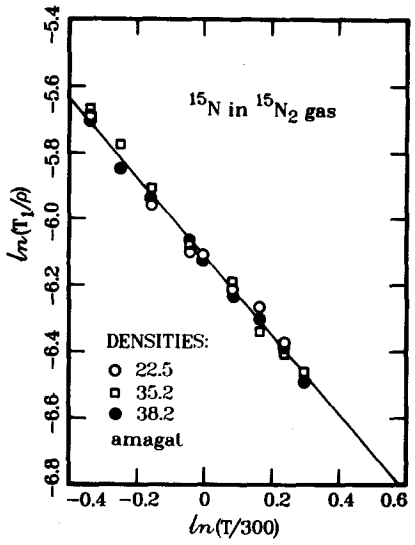

FIG. 2. Typical data showing the temperature dependence of (T_1/ρ) for several samples of pure N_2 gas.

TABLE II. Cross sections for rotational angular momentum transfer for ^{15}N in N_2 with various buffers.[a] $\sigma_J(T) = \sigma_J(300\text{ K})\cdot(T/300)^{-m} \simeq (300/T)\sigma_J(300\text{ K})[1 + a_1(T - 300)]$.

Buffer	m	$\sigma_J(300)$ (Å^2)	$a_1 \times 10^2$ (deg^{-1})
CH_4	0.60 ± 0.06	13.6 ± 0.4	1.7 ± 0.2
N_2	0.70 ± 0.03	14.9 ± 0.4	1.54 ± 0.14
O_2	0.87 ± 0.06	14.7 ± 0.6	0.6 ± 0.3
CO	0.67 ± 0.09	15.0 ± 0.9	1.58 ± 0.47
Ar	0.74 ± 0.04	15.9 ± 0.8	1.42 ± 0.21
HCl	0.98 ± 0.02	22.7 ± 0.6	...
CF_4	0.88 ± 0.04	30 ± 1	1.1 ± 0.4
Kr	0.74 ± 0.05	18.1 ± 0.5	1.62 ± 0.27
Xe	0.77 ± 0.05	19.8 ± 0.5	1.46 ± 0.33

[a] Temperature ranges are the same as in Table I.

Gordon's theory[16]

$$(T_1/\rho) = (3/2\langle J(J+1)\rangle C_1^2)\bar{v}\sigma_J(T), \quad (4)$$

where $\bar{v}$ is the mean relative velocity $(8kT/\pi\mu)^{1/2}$. Taking $\langle J(J+1)\rangle$ to be the classical limit kT/B_0 is in error by less than 1/2% at 200 K and is an even better approximation at 400 K. The rotational constant is 1.8658 cm^{-1},[17] and the spin-rotation constant (C_1) used for ^{15}N in N_2 is 20.0 ± 0.01 kHz from shielding measurements.[18] The spin-rotation constant has been measured by molecular beam magnetic resonance spectroscopy (22.0 ± 1.0 kHz),[19] but is less precise than the value derived from the absolute shielding scale based on ^{15}N in NH_3. The cross section $\sigma_J(T)$ is interpreted classically as[16]

$$\sigma_J(T) = (1/2\langle J^2\rangle^T)\int_0^\infty \langle(\Delta\mathbf{J})^2\rangle 2\pi b\, db, \quad (5)$$

where $\Delta\mathbf{J}$ is the change in the rotational angular momentum vector of the N_2 molecule by a collision and $\langle\ \rangle$ denotes the average over the initial distribution of internal states before a collision and the initial distribution of relative velocities. These cross sections are plotted in Fig. 3.

Deviation of (T_1/ρ) from $T^{-3/2}$ behavior implies that the collision integral $\frac{1}{2}\int\langle\Delta\mathbf{J}^2\rangle 2\pi b\, db$ is temperature dependent. If we factor out the T^{-1} dependence which is implicit in $1/\langle J^2\rangle^T$ in Eq. (5), the residual temperature dependence of the collision integral can be determined to the extent shown in Fig. 4. A straight line adequately describes these curves:

$$(T/300)\sigma_J(T) = \sigma_J(300)[1 + a_1(T - 300)], \quad (6)$$

with the values of the coefficient a_1 given in Table II. For each N_2/buffer pair, the collision integral increases with increasing temperature, a behavior also observed for CO_2–CH_4, CO_2–N_2, CO_2–Ar, and CO_2–Kr.[14]

DISCUSSION

Of the $^{15}N_2$ modifications only ortho N_2 has a resultant nuclear spin ($I = 1$), hence only the influence of collisions

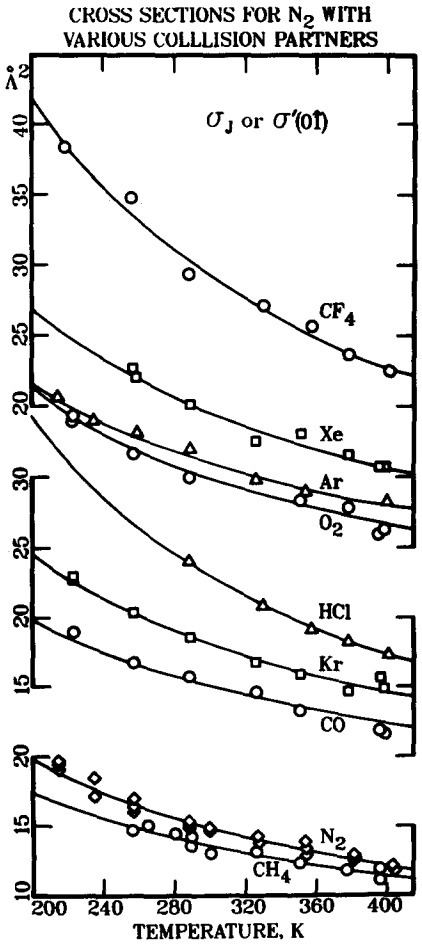

FIG. 3. The temperature dependence of the cross section $\sigma_J(T)$, for N_2 with various collision partners.

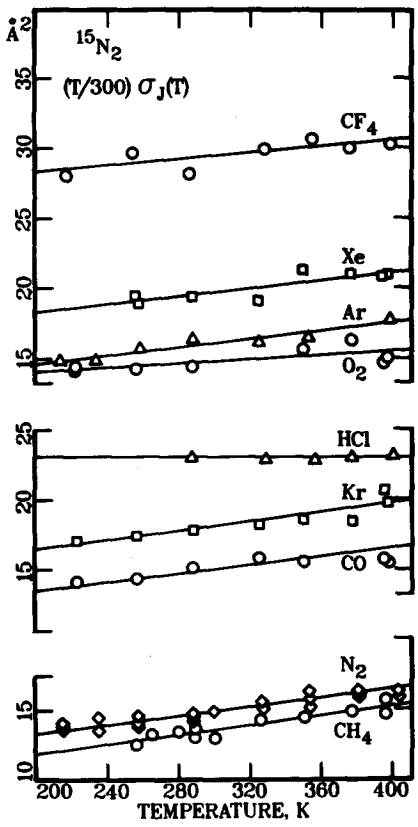

FIG. 4. The temperature dependence of $(1/2\langle J^2\rangle_{300})\int_0^\infty \langle\Delta\mathbf{J}^2\rangle 2\pi b\, db$ is given by $(T/300)\,\sigma_J(T)$.

TABLE III. Geometric cross sections and collision efficiencies at room temperature for N_2 with various buffers.

Buffer	σ_{geom} (Å^2)[a]	σ_J/σ_{geom}
CH_4	41.92	0.32
N_2	41.44	0.36
O_2	38.84	0.38
CO	41.00	0.37
Ar	38.05	0.42
HCl	38.17	0.58
CF_4	53.59	0.56
Kr	41.60	0.44
Xe	44.75	0.44

[a] The geometric cross section $\sigma_{geom} = \pi r_0^2$ where r_0 are taken from G. C. Maitland, M. Rigby, E. B. Smith, and W. A. Wakeham, *Intermolecular Forces, Their Origin and Determination* (Clarendon, Oxford, 1981) (Table A3.2) except for N_2–HCl and N_2–CO which were taken as arithmetic means of r_0 for like pairs, r_0(CO–CO) = 3.592 Å [R. D. Trengove, J. L. Robjohns, and P. J. Dunlop, Ber. Bunsenges. Phys. Chem. **88**, 450 (1984)] and r_0(HCl–HCl) = 3.339 Å [A. F. Turfa and R. A. Marcus, J. Chem. Phys. **70**, 3035 (1979)].

on the ortho molecules can be detected. However, unlike H_2 in which the ortho and para modifications can individually be observed, in a heavy diatomic molecule such as N_2 the separate contributions from the various spin-symmetry modifications are undetectable.

The geometric cross sections $\sigma_{geom} = \pi r_0^2$ for each N_2/buffer pair are given in Table III. The ratio σ_J/σ_{geom} describes the efficiency of collisions in causing changes in the rotational angular momentum of the N_2. The ratio is less than 1; every two or three "hard-sphere" collisions causes a change in rotational angular momentum. The collision efficiency increases with increasing polarizability of the buffer, with a few exceptions. This indicates that these data are sensitive to the anisotropy of dispersion forces. At the same time, all cross sections are smaller than the geometric cross section which implies that considerable information about the short range anisotropy is included in σ_J. The highest efficiency is for N_2–HCl collisions, which can be explained by contributions from the electrostatic interaction between the large HCl dipole moment and the N_2 quadrupole moment which falls off as R^{-4} compared to dispersion forces which fall off as R^{-6}.[20] N_2 is a less effective collision partner than CO_2, because CO_2 has a larger electric quadrupole moment and is more polarizable than N_2. Geometric constraints also make the N_2–CO_2 potential more anisotropic than the N_2–N_2 potential.

The relaxation time of ^{14}N nuclei in pure N_2 gas has been measured as a function of density and temperature.[12] For this isotope, the dominant relaxation mechanism is the intramolecular quadrupolar coupling mechanism. At low densities, in the extreme narrowing limit, theory predicts and experiments confirm that T_{1q} is proportional to density[16]:

$$T_{1q} = \frac{160I^2(2I-1)}{3(2I+3)}(\hbar/eqQ)^2\rho\bar{v}\sigma_\theta, \tag{7}$$

where eqQ is the nuclear quadrupole coupling constant. In the classical limit, the cross section designated as σ_θ is entirely due to reorientation and is given by[16]

$$\sigma_\theta = \int_0^\infty (3/2)\langle 1-\cos^2\theta\rangle 2\pi b\,db. \tag{8}$$

θ is the angle through which the rotational angular momentum vector **J** is rotated by one collision. The average $\langle\ \rangle$ is over the internal states of the molecules, but not their relative velocities. In the semiclassical theory, σ_θ also includes (to a minor extent) contributions due to changes in J value.[21] This quadrupolar relaxation cross section, σ_θ, provides information on the anisotropy of the potential which is complementary to our spin-rotation cross section σ_J.

In the semiclassical theory of spin relaxation, contributions to the thermal average σ_J are J dependent. For low J states both strong and weak collisions contribute to the average, producing *large* sigma matrix elements which depend primarily upon weak collisions which are dominated by the attractive potential. For high J states only strong collisions have sufficiently rapidly varying potentials to produce transitions, thus the sigma matrix elements are *smaller* and depend primarily upon strong collisions dominated by the repulsive anisotropy.[21] Semiclassical calculations reveal that both the quadrupolar and the spin-rotation mechanisms are dominated by elastic collisions.[21] However, the spin rotation mechanism weights high J states more heavily (the weights grow roughly as J^2 times the population weighting in the averaging which leads to the spin-rotation cross section). The quadrupolar mechanism depends primarily on reorientation behavior of the low J states. The weighting factors are $\frac{2}{5}, \frac{2}{9}, \frac{4}{13}, \frac{20}{77}, \ldots$ for $J = 1, 2, 3, 4, \ldots$ and approaching $\frac{1}{4}$ for high J and the classical limit. Thus, the low J states are weighted more than strict population weighting in quadrupolar relaxation. For high J states (which are more highly weighted by the spin rotation mechanism) collisions strong enough to reorient the angular momentum vector occur at lower impact parameters which also cause inelastic transitions. For low J states, grazing collisions can cause molecular reorientation without changing J. Thus, the spin-rotation mechanism includes more contributions from inelastic collisions than the quadrupolar mechanism. Because sigma matrix elements for low J states depend primarily on the attractive part and high J states on the repulsive part of the potential, the ratio of these two cross sections depends on the detailed form of the anisotropic part of the potential. If only elastic collisions are included in the classical limit, the cross section σ_θ goes as $(3/2)\langle 1-\cos^2\theta\rangle$ whereas σ_J goes as $\langle 1-\cos\theta\rangle$.[16] Kinetic theory cross sections corresponding to the reorientation of the **J J′** tensor [such as $\sigma(02)$ or σ_θ] are larger than the cross sections corresponding to the reorientation of the **J** vector [such as $\sigma(01)$ or σ_J] by factors such as 3/2 or 7/4 at the high temperature limit in classical theory.[22] Experimental evidence supports this, we find the cross section for $^{14}N_2$ relaxation is significantly larger than that for $^{15}N_2$, σ_θ:σ_J is 1.7:1 at room temperature. This is not atypical compared to 1.38:1 in ClF,[23] or σ_{NRA}:σ_J = 1.82:1 in NH_3[24] or $\sigma(02)$:σ_J = 1.85:1 for CH_4 and 1.6:1 in CF_4,[25] where $\sigma(02)$ and σ_{NRA} are reorientation cross sections which are related to σ_θ in the classical limit.

Sound absorption also depends on the anisotropy of the

TABLE IV. Comparison of experimental effective cross sections for N_2–N_2.

Experiment	Dominant dynamic variable	Cross section[a]	Room T value (Å^2)	T dep.	Reference
Sound absorption	J^2 change	$\sigma(0001)$ or σ_{rot}	7.6 ± 0.8 10.4	yes	29 26
Viscosity	WW'	$\sigma(20)$	35.0 ± 0.4	yes	25
Viscomagnetic effect	**J J′** tensor polarization	$\sigma(02\pi)$	23.7 ± 0.9	yes	25
Depolarized Rayleigh	**J J′** tensor polarization	$\sigma(0\hat{2})$[b] or σ(DPR)	34.4 ± 0.6,35.5		30,1
NMR relaxation (quadrupolar)	**J J′** tensor polarization[c]	$\sigma'(0\hat{2})$ or σ_θ	26,[d] 39	yes	12,1
NMR relaxation (spin rotation)	**J** vector polarization[e]	$\sigma'(0\hat{1})$ or σ_J(SR)	14.9 ± 0.4	yes	This work
Magnetic effect on heat conductivity	**W J J′** polarization	$\sigma(12q)$	43	yes	31

[a] Notation is defined in Ref. 3 for the traditional approach, and in Ref. 1 for the recently introduced treatment involving unknown scalar factors.

[b] The hat indicates normalization by division by its constituent vectors. Thus, while $\sigma'(02) = \frac{3}{4}\langle \frac{2}{3}J^4 - [(\mathbf{J}\cdot\mathbf{J}')^2 - \frac{1}{3}J^2J'^2]\rangle$ (in the traditional approach), the normalized value is $\sigma'(0\hat{2}) = \frac{3}{2}\langle 1 - ((\mathbf{J}\cdot\mathbf{J}')^2/J^2J'^2)\rangle = \frac{3}{2}\langle 1 - \cos^2\theta\rangle$.

[c] In the classical limit, the cross sections from depolarized Rayleigh, depolarized Raman scattering, and the NMR quadrupolar spin relaxation are all due entirely to **J J′** tensor polarization (molecular reorientation) and all correspond to $(3/2)\langle 1 - \cos^2\theta\rangle$. However, in semiclassical theory this is no longer true (Ref. 21). In the low density limit (but still in the extreme narrowing region), the sigma matrix elements corresponding to depolarized Raman linewidths and the quadrupolar relaxation are affected strongly by reorientation but to a minor extent also by changes in J value.

[d] The error associated with this value is somewhat large due to the considerable deviation from linearity of T_1 vs ρ for the high densities used in the original experiments.

[e] In semiclassical theory this includes not only reorientation of the **J** vector but also changes in J magnitude, i.e., off-diagonal sigma matrix elements (Ref. 21). In classical theory, on neglect of inelastic contributions this reduces to $\sigma_J = \int_0^\infty \langle 1 - \cos\theta\rangle 2\pi b\, db$ (Ref. 16), which is identical to $\sigma'(0\hat{1})$ of Beenakker *et al.* (Ref. 2).

potential. It has been shown that sound absorption is due only to those collisions which are strong enough to change the magnitude of the J vector,[21] yielding information primarily about the angular dependence of the potential at short distances where the interactions are strongest. The cross sections from these sound absorption measurements [$\sigma(100)$ or σ_{rot}] should thus be smaller than the spin-rotation or the quadrupolar relaxation cross sections:

$$\sigma_\theta(q) > \sigma_J(\mathrm{SR}) > \sigma_{rot}.$$

For N_2 gas the respective values are 26,[12] 14.9 (this work), and 10.4 Å^2,[26] which furnish information on the angle dependence of the N_2–N_2 potential at long range, a combination of long and short range, and very short range, respectively. For N_2–Ar and N_2–Xe the sound absorption cross sections are also smaller than the spin-rotation relaxation cross sections (11–16 Å^2 vs 16 Å^2 for N_2–Ar and 7.6–11.6 Å^2 vs 19.8 Å^2 for N_2–Xe).[26] The decreased efficiency of N_2–Xe collisions (0.17–0.26) compared to N_2–Ar (0.28–0.4) in the sound absorption experiments can be explained as being due to the very large mass mismatch in the pair, a more important factor for J-changing collisions in sound absorption than reorientations of **J** in spin-rotation relaxation.

The cross sections from NMR are compared with others derived from various experiments in pure N_2 in Table IV and Fig. 5. Some experiments depend on several different cross sections at once (these are not included in Table IV). The experiments with the most straightforward interpretation are those characterized by a single cross section, i.e., a single frequency-independent relaxation time, as is the case in T_1(SR) or $T_1(q)$ in N_2 in the extreme narrowing limit, in depolarized Rayleigh scattering, or in sound absorption. Even so, there are problems in interpretation of the latter experiments for N_2, the line shape of the depolarized Rayleigh line does not transform into a single exponential and the sound absorption coefficient is frequency dependent.[27] For some systems such as those chosen in this study, cross sections from NMR measurements in the gas phase have the advantage of having a well-defined single relaxation time and no frequency dependence in the extreme narrowing lim-

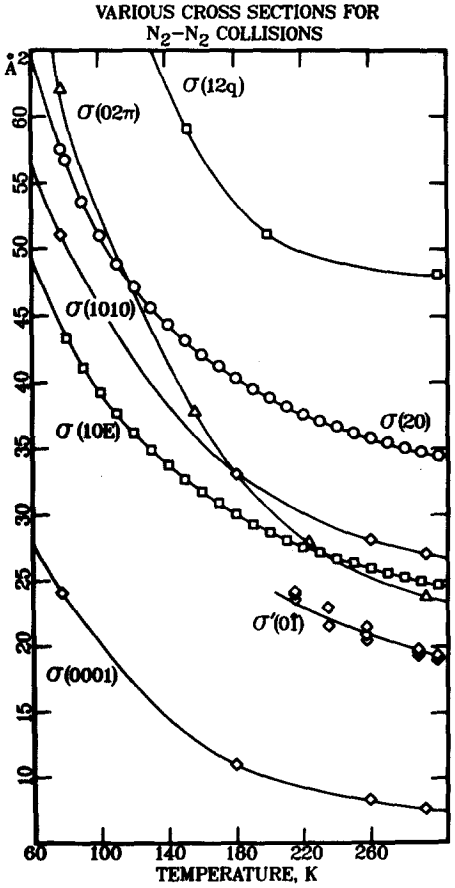

FIG. 5. The temperature dependence of cross sections defined in Table IV for N_2.

it. This leads to a single well-defined cross section rather than a combination of cross sections. Furthermore, the intramolecular interaction which is responsible for the spin relaxation is well understood so that the J-magnitude dependence of the individual sigma matrix elements is well defined, unlike other observables such as the viscomagnetic effect.[28] Another advantage of NMR measurements is that cross sections for unlike pairs are just as easy to obtain as for like pairs, since no buffer–buffer collisions contribute.

CONCLUSIONS

The cross sections for rotational angular momentum transfer (σ_J) found in this study provide information on the range of anisotropic intermolecular forces. The small N_2–CO, N_2–N_2, and N_2–O_2 cross sections indicate contributions from relatively short range torques in inelastic and elastic collisions and contain information about repulsive branch anisotropy, while the larger N_2–CF_4 and N_2–Xe cross sections suggest important contributions from the anisotropy in the dispersion terms. For nearly all molecular pairs in this study the observed temperature dependence of the cross section differs from T^{-1} so that the cross sections measured at different temperatures contain independent information. For N_2–N_2 several cross sections already available from different experiments provide complementary information about the intermolecular potential.

ACKNOWLEDGMENT

This research was supported in part by the National Science Foundation (Grant No. CHE85-05725).

[1] H. Van Houten, L. J. F. Hermans, and J. J. M. Beenakker, Physica A **131**, 64 (1985).
[2] J. J. M. Beenakker, H. F. P. Knaap, and B. C. Sanctuary, AIP Conf. Proc. **11**, 21 (1973).
[3] A. F. Turfa, J. N. L. Connor, B. J. Thijsse, and J. J. M. Beenakker, Physica A **129**, 439 (1985).
[4] A. van der Avoird, P. E. S. Wormer, and A. P. J. Jansen, J. Chem. Phys. **84**, 1629 (1985); F. Visser, P. E. S. Wormer, and P. Stam, *ibid.* **79**, 4973 (1983); R. M. Berns and A. van der Avoird, *ibid.* **72**, 6107 (1980); F. Mulder, G. van Dijk, and A. van der Avoird, Mol. Phys. **39**, 407 (1980); M. C. van Hemert and R. M. Berns, J. Chem. Phys. **76**, 354 (1982).
[5] S. L. Price, Chem. Phys. Lett. **79**, 553 (1981); C. Nyeland, J. Phys. Chem. **88**, 1216 (1984); N. Corbin, W. J. Meath, and A. R. Allnatt, Mol. Phys. **53**, 225 (1984).
[6] M. S. H. Ling and M. Rigby, Mol. Phys. **51**, 855 (1984).
[7] E. C. Morris and R. G. Wylie, J. Chem. Phys. **79**, 2982 (1983).
[8] M. Deraman, J. C. Dore, and J. G. Powles, Mol. Phys. **52**, 173 (1984); P. A. Egelstaff, R. K. Hawkins, D. Litchinsky, P. A. De Longi, and J. B. Suck, *ibid.* **53**, 389 (1984).
[9] A. DeSantis and M. Sampoli, Mol. Phys. **51**, 97 (1984); A. DeSantis, M. Sampoli, P. Morales, and G. Signorelli, *ibid.* **35**, 1125 (1978); A. DeSantis, E. Moretti, and M. Sampoli, *ibid.* **46**, 1271 (1982).
[10] M. Moon and D. W. Oxtoby, J. Chem. Phys. **84**, 3830 (1986); N. W. B. Stone, L. A. A. Read, A. Anderson, I. R. Dagg, and W. Smith, Can. J. Phys. **62**, 338 (1984); A. Rastogi and P. R. Lowndes, J. Phys. B **10**, 495 (1977); J. D. Poll and J. L. Hunt, Can. J. Phys. **59**, 1448 (1981).
[11] K. S. Jammu, G. E. St. John, and H. L. Welsh, Can. J. Phys. **44**, 797 (1966); R. D. Trengrove and P. J. Dunlop, Physica A **115**, 339 (1982); E. Mazur, H. J. Hijnen, L. J. F. Hermans, and J. J. M. Beenakker, *ibid.* **123**, 412 (1984).
[12] P. A. Speight and R. L. Armstrong, Can. J. Phys. **47**, 1475 (1969); N. S. Golubev, A. I. Burshtein, and S. I. Temkin, Chem. Phys. Lett. **91**, 139 (1982).
[13] C. J. Jameson, A. K. Jameson, and S. M. Cohen, J. Chem. Phys. **62**, 4224 (1975).
[14] C. J. Jameson, A. K. Jameson, N. C. Smith, and K. Jackowski, J. Chem. Phys. **86**, 2717 (1987).
[15] R. L. Vold, J. S. Waugh, M. P. Klein, and D. E. Phelps, J. Chem. Phys. **48**, 3831 (1968).
[16] R. G. Gordon, J. Chem. Phys. **44**, 228 (1966).
[17] D. Steele, E. R. Lippincott, and J. T. Vanderslice, Rev. Mod. Phys. **34**, 239 (1962).
[18] C. J. Jameson, A. K. Jameson, D. Oppusunggu, S. Wille, P. M. Burrell, and J. Mason, J. Chem. Phys. **74**, 81 (1981).
[19] M. R. Baker, C. H. Anderson, and N. F. Ramsey, Phys. Rev. A **133**, 1533 (1964).
[20] A. D. Buckingham, Adv. Chem. Phys. **12**, 107 (1967).
[21] W. B. Nielsen and R. G. Gordon, J. Chem. Phys. **58**, 4131, 4149 (1973).
[22] H. Moraal, Z. Naturforsch. Teil A **28**, 824 (1973).
[23] K. T. Gillen, D. C. Douglass, and J. E. Griffiths, J. Chem. Phys. **69**, 461 (1978).
[24] C. Lemaire and R. L. Armstrong, J. Chem. Phys. **81**, 1626 (1984).
[25] A. L. J. Burgmans, P. G. van Ditzhuyzen, H. F. P. Knaap, and J. J. M. Beenakker, Z. Naturforsch. Teil A **28**, 835 (1973).
[26] P. G. Kistemaker and A. E. Devries, Chem. Phys. **7**, 371 (1975).
[27] R. A. J. Keijser, K. D. van den Hout, and H. F. P. Knaap, Phys. Lett. A **42**, 109 (1972).
[28] R. F. Snider, J. Chem. Phys. **81**, 3482 (1984).
[29] G. J. Prangsma, A. H. Alberga, and J. J. M. Beenakker, Physica **64**, 278 (1973).
[30] R. A. J. Keijser, K. D. van den Hout, M. de Groot, and H. F. P. Knaap, Physica **75**, 515 (1974).
[31] B. J. Thijsse, W. A. P. Denissen, L. J. F. Hermans, H. F. P. Knaap, and J. J. M. Beenakker, Physica A **97**, 467 (1979).